DYNAMIC SIMULATION OF MONO-TUBE CAVITY RECEIVERS FOR DIRECT STEAM GENERATION

José Zapata[1], John Pye[2], Keith Lovegrove[3]

[1]BEng(hons), PhD student, Research School of Engineering (RSE), Australian National University (ANU), Canberra, ACT, 0200, Australia, Phone: +61-2 6125 3072, jose.zapata@anu.edu.au

[2] BE/BSc, PhD, Lecturer, RSE, ANU. [3] BSc(Hons),PhD, Assoc. Prof., RSE, ANU.

Abstract

The ANU 500 m^2 dish has been in operation since 2010 with a mono-tube steam cavity receiver, the SG4 system for the production of steam used for electricity generation. Dynamic modelling of this system is crucial for achieving robust control and optimised performance.

This paper presents ongoing work with the dynamic modelling and simulation of a mono-tube steam cavity receiver for direct steam generation. A ray-tracing study of the heat flux distribution inside the steam receiver is used to spatially refine the model and improve its accuracy for large transients. A subdivision of the dynamic model into sub-models is proposed and a simulation is presented to support this approach. Initial modelling results show qualitative agreement with experimental data, and the model will be progressively expanded to cover the full range of possible operational scenarios.

Keywords: Parabolic Dish, Direct Steam Generation, Dynamic Simulations,

1 Introduction

Since the completion of the 500 m^2 SG4 dish concentrator system in 2009 [1], the Solar Thermal Group at the Australian National University (ANU) has been working on operating the dish with a mono-tube boiler direct steam generating receiver. The motivation for investigation of direct steam generation is that dish systems for intended deployment in large arrays of dishes, with steam directed to a central large steam turbine power block. The steam produced within the receiver on the SG4 dish is fed to an experimental steam system that includes a 4 cylinder steam engine coupled with a 3 phase generator. This paper describes ongoing research on the dynamic modelling of the mono-tube receiver and the development of optimised control systems.

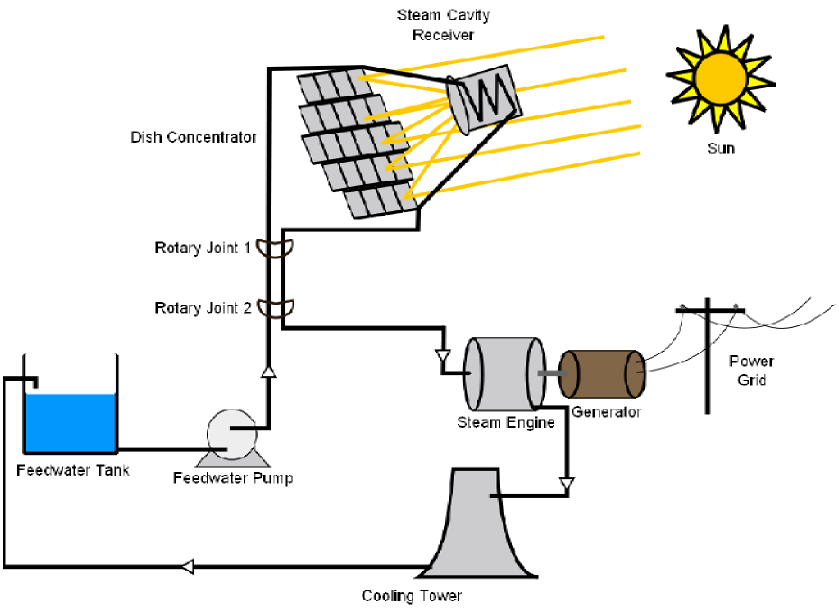

Fig.1. Diagram of the Experimental System at the Australian National University

2 Experimental System

2.1 Overall Description

The experimental system consists of a feed-water tank and pump, the mono-tube steam cavity receiver [2] mounted to the 500 m^2 dish receiver supports, a modified steam engine coupled to an electrical generator, a cooling tower and associated piping.

The steam system is installed in a shipping container approximately 50m from the base of the dish. Water is fed to the receiver using a reciprocating pump from a reservoir tank using a feed water line. A steam line connected to the receiver outlet transports superheated steam via rotary joints to the ground and then to a 4 cylinder steam engine, there is also the option of releasing some or all of the steam from a control valve on the back of the receiver. The engine powers a 50kW 3-phase generator. Exhaust vapour is cooled and condensed and then fed back to the water tank for reuse. The thermal output of the system exceeds the capacity of the steam engine and therefore a vent valve has been installed at the receiver outlet to vent a portion of the superheated steam to atmosphere.

2.2 System Measurements

The steam cavity receiver is fitted with pressure transducers at the inlet and exit and several thermocouples measuring tube temperatures at various lengths along the receiver length. Feed water properties such as pressure, temperature and mass flow rate are also measured. The pressure and temperature of the steam feeding the engine are measured and also ambient conditions such as direct normal irradiance, wind speed and ambient temperature are also measured. A detailed description of the measurements of the system and data collection is reported in an associated paper in these proceedings[3].

3 Dynamic modelling

A dynamic model of the steam cavity receiver has been developed and previously described by the authors in the previous year's proceedings [2]. This model is a first-principles representation of the receiver using a moving boundary formulation[4]. Equations governing the conservation of mass, energy and momentum in the fluid plus an energy balance of the tube wall describe the dynamic behaviour of the evaporator. Phase changes of water are handled by defining three flow regions inside the evaporator, a sub-cooled region, a saturated region and a superheated region.

3.1 Influence of Heat Flux Distribution in the Cavity Receiver

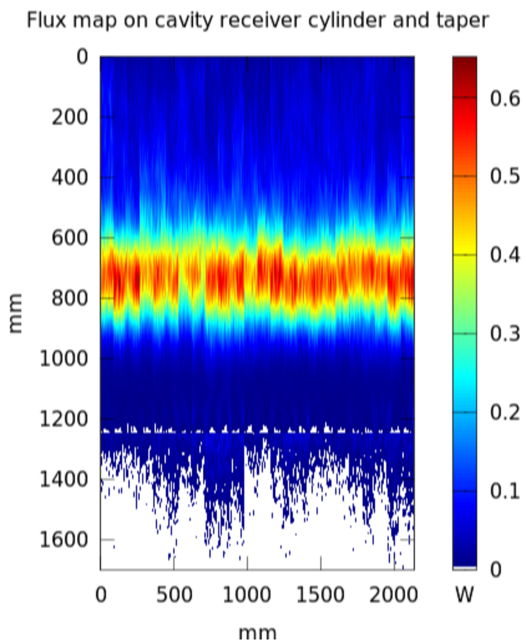

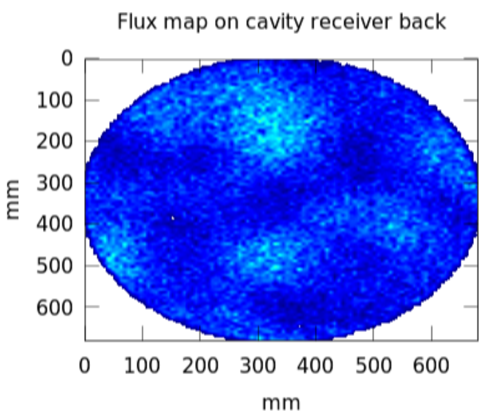

Fig.2. Ray-trace map of 500 m^2 dish flux onto the inner surface of steam cavity receiver

A ray-tracing model of the SG4 500 m^2 and how its concentrated heat flux is distributed on the steam cavity receiver surface has been performed using OPTICAD 10[5]. The ray tracing study has provided an estimation of the heat flux distribution on the cavity receiver's inside surface. Ongoing work in this area is focused on the validation of this ray-tracing calculation by measurements of dish surface and incoming flux.

Figure 2 shows the distribution of incident radiation within the receiver surface. The figure on the right has units in mm and each pixel of the map has its intensity in W mapped to a colour. The vertical axis represents cavity depth, with 0 at the deepest, and 1256 the transition from cylindrical to conical in shape. The figure on the right depicts the irradiance map on the back of the disk.

Following on from this, a heat flux profile has been calculated as a function of the cavity receiver tube length and compared to temperature measurements of the cavity receiver operating at steady-state, during the month of May 2011. This steady state was maintained for over 2 hours, with a feed-water mass flow of 120 g/s and an average insolation of 906 W/m2. The pressure at the receiver outlet fluctuates around 3.8 MPa.

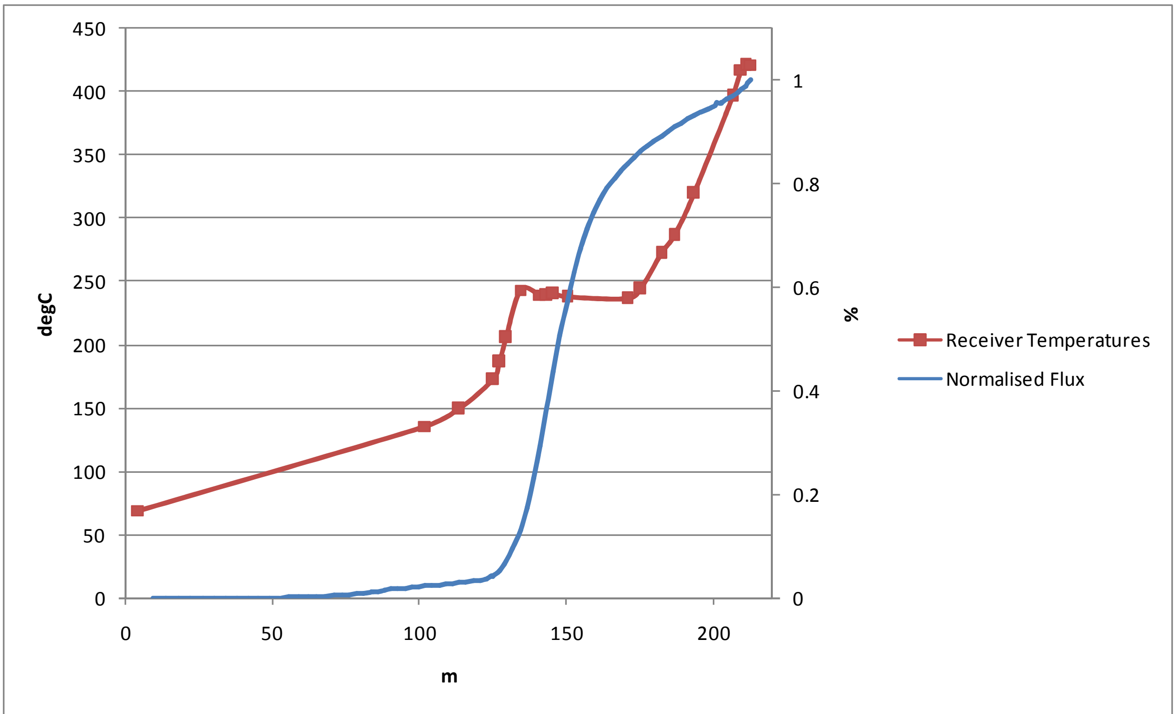

Fig.3. Temperature profile of steam cavity receiver at steady state and normalised cumulative flux over the receiver surface as a function of receiver tube length

Figure 3 shows on one scale, the water temperature profile for the steam cavity receiver during the steady state run. A region of sub-cooled water can be observed in the first 135 m of tube and a region of saturated water between 135 and 170 m approximately. Finally a region of superheated steam can be observed in the last 45 m of tube. On the other scale is the cumulative flux prediction from ray tracing. Also three regions of flux can be distinguished. Firstly over the first 120 m of tube, approximately 6% of the total flux is captured. In the next segment, approximately 67% of the total flux hits the subsequent 42 m of piping. In the final segment of approximately 65 m, the remaining 27% of flux is observed.

There is a strong relation between temperature/enthalpy change and local incident flux on the receiver tubes. As the water traverses through tube sections with low heat flux, the temperature change is small, whereas an increase in heat flux per unit of length drives the heating of water quickly into boiling. Once the fluid is saturated, the temperature depends on the tube pressure. As pressure drops are experienced within the receiver, the saturation temperature drops slightly. The relatively short length of the boiling region also indicates that high heat transfers occur due to the high local heat flux profile. The heat flux decreases before the end of the boiling region but it is sufficient to make the fluid superheat. The temperature rise of the superheated steam is steady along the length of the receiver, which compares well with the cumulative flux profile for the last section of piping.

3.2 Model subdivision

In the dynamic model of the cavity receiver, the heat flux incident on the tube is assumed to be equally distributed along the control volume's length. This has a significant effect on the rate of change of energy in the fluid and if it is not considered in the model, there may be severe discrepancies between modelled and measured boiling profiles.

Several instances of the model can be created and connected in series, so that the outlet fluid properties of one instance are the inlet properties of the next. This allows versatility to subdivide the receiver geometry into regions of comparable heat flux, pipe geometry and other parameters, such as convective and reflective losses, thus increasing the accuracy of the overall model. On the other hand, more model instances results in a greater number of calculations, it departs from a compact description of the system that can be used for control algorithm design and forgoes the simplicity of a moving boundary approach.

It is for this reason that the subdivision of the dynamic model into three instances is proposed. In accordance with the estimated ray tracing heat flux profile and its good agreement with experimental data, three regions of heat flux can be identified. For each heat flux region, the assumption that the flux is evenly distributed is more sensible, and when applied to the moving-boundary form.

The following table presents a summary of the proposed compound model.

Model Instance	**Length [m]**	**Heat Flux [%]**	**Expected flow regions (sub-models of two-phase flow)**	**Tubing Type**
Cavity Receiver Front-Inlet	123	6	Sub-cooled only.	16mm steel
Middle of receiver	41	67	Sub-cooled only, Sub-cooled & Saturated, Sub-cooled & Saturated & Superheated	¾ inch steel
Cavity Receiver Back – Outlet.	65	27	All above plus Saturated only, Saturated & Superheated, Superheated only	¾ inch steel

Table 1. Multiple instances of moving boundary model, based on heat flux profile in receiver tube

It is observed that the first instance, for the first section of cavity receiver tube, is highly unlikely to ever represent a two-phase flow, for the intended operating conditions of the system. There first section of pipe comprises the entire portion of the cavity receiver tube that uses 16 mm tubing, which is also considered as a factor influencing the decision to consider it a single section.

The second region, with the most flux per length, is likely to experience the largest transients and therefore dominate the behaviour of the receiver. This is where boiling flow will occur around a steady state condition, and the outlet may be superheated for the lower end of permissible mass flow rates.

The third region, representing the last section of tube before the outlet presents the most evenly distributed heat flux per length, and the types of flow represented, depend on the previous region. This instance of the model will represent the most diverse combination of sub-cooled, saturated and superheated flow. Around steady-state however, it may only model superheated flow or saturated and superheated flow.

3.3 Simulation Environment

The receiver model has been programmed in Matlab and simulated using a Runge-Kutta (2,3) algorithm based solver [6]. A total of 9 state equations are calculated at each time step, as well as thermodynamic properties of the fluid using the IAPWS IF97 standard formulation generated by the function XSteam for

Matlab[7]. A switching algorithm has been built into the simulation, enabling the model to switch between two-phase flow regimes, such as start up and operating conditions[8].

Physical parameters such as dimensions, heat transfer coefficients and receiver pipe dimensions determine the dynamic behaviour of the model. Inputs such as ambient temperature, direct normal irradiance, average dish reflectivity and mass flow are used to calibrate the model to match it to experimental results.

3.4 Simulation of middle sub-model of steam cavity receiver

A transient simulation of the behaviour of the middle receiver section during start-up is presented. The simulation considers the first receiver section behaviour as a starting condition, and its output is used to simulate the third and final region of the receiver, which mostly completes the superheating process.

In experimental runs, it is typical to run the experiment with a fixed and relatively high mass-flow at the start, to protect the conical section of the cavity receiver from thermal shock when initially focusing the sun. Once the heat flux is aligned with the cavity, the mass flow is reduced to a value in accordance to the desired outlet temperature.

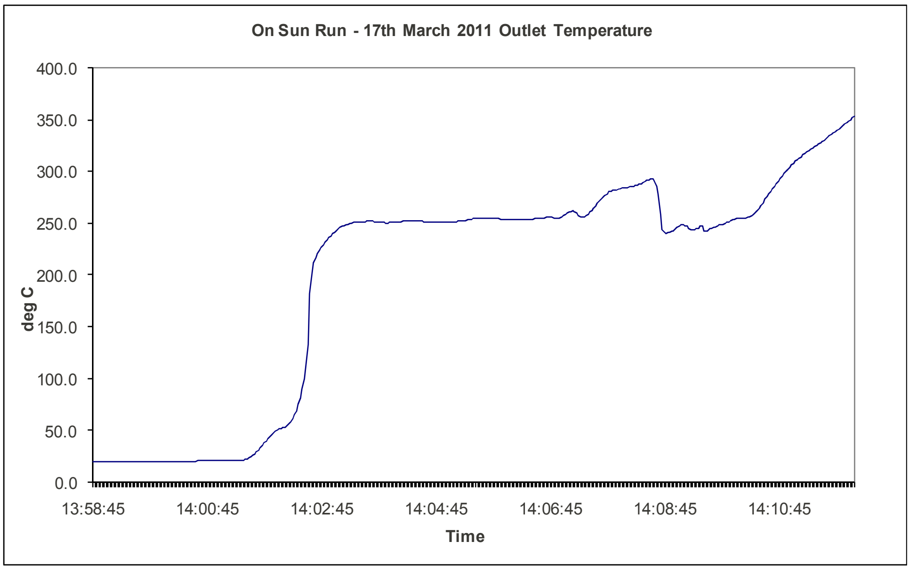

Fig.4. Steam receiver outlet temperature during experimental run in March 2011, at the time when the dish concentrator focuses the sun.

Figure 4 depicts an experimental run of the dish system with the steam cavity receiver. In this run the mass flow has been kept stable at 150g/s until the dish is focused and then reduced to 110g/s to increase the outlet temperature. The outlet temperature transitions rapidly from ambient temperature to approximately 255 °C. At this point, the fluid enters saturation, for a pressure of approximately 4 MPa and for this reason, the temperature does not increase, although the fluid thermal energy continues to increase. The outlet temperature resumes its increase once the outlet state is of saturated vapour to eventually settle at a superheated steam temperature.

Figure 5 shows a dynamic simulation of the middle section of the receiver under this conditions. It is taken from the point where the receiver is focused to the sun, the outlet temperature is 50 °C and mass flow is 110g/s. All environmental conditions such as wind, direct normal irradiance and ambient temperature have been assumed constant. Only the first 500 seconds are presented due to the fact that the middle section settles to a 2 region flow regime for this conditions. The authors are continuing to work on a full scale of the model where the transition from saturation to superheat is depicted.

The top diagram shows the lengths of sub-cooled and saturated liquid, relative to the middle section's length. It shows that the beginning, the sub-cooled region occupies the entire section of receiver, and it is the case until the water enters saturation, where the saturated region gains space at the outlet at approximately 40s.

Due to the amount of energy absorbed by the water, the saturated region grows rapidly, occupying almost 30m of section. In steady state, there is agreement between the simulation's sub-cooled length approximately 13m of the section and the steady state temperature profile presented earlier.

The middle figure shows the pressure in this tube section and the outlet enthalpy of the water for this section. There is a sharp increase in pressure due to the increase in energy in the fluid and the limited ability to expand within the cavity receiver. The enthalpy increase is steady and similar to a first order differential equation, where the increase is affected principally by the combined tube and water masses and their respective heat capacities. In both plots, there is a sharp discontinuity at the transition from sub-cooled only to sub-cooled and saturated. The cause of this is not known by the authors, but it is more likely that this is related to the simulation method rather than a boiling flow phenomenon.

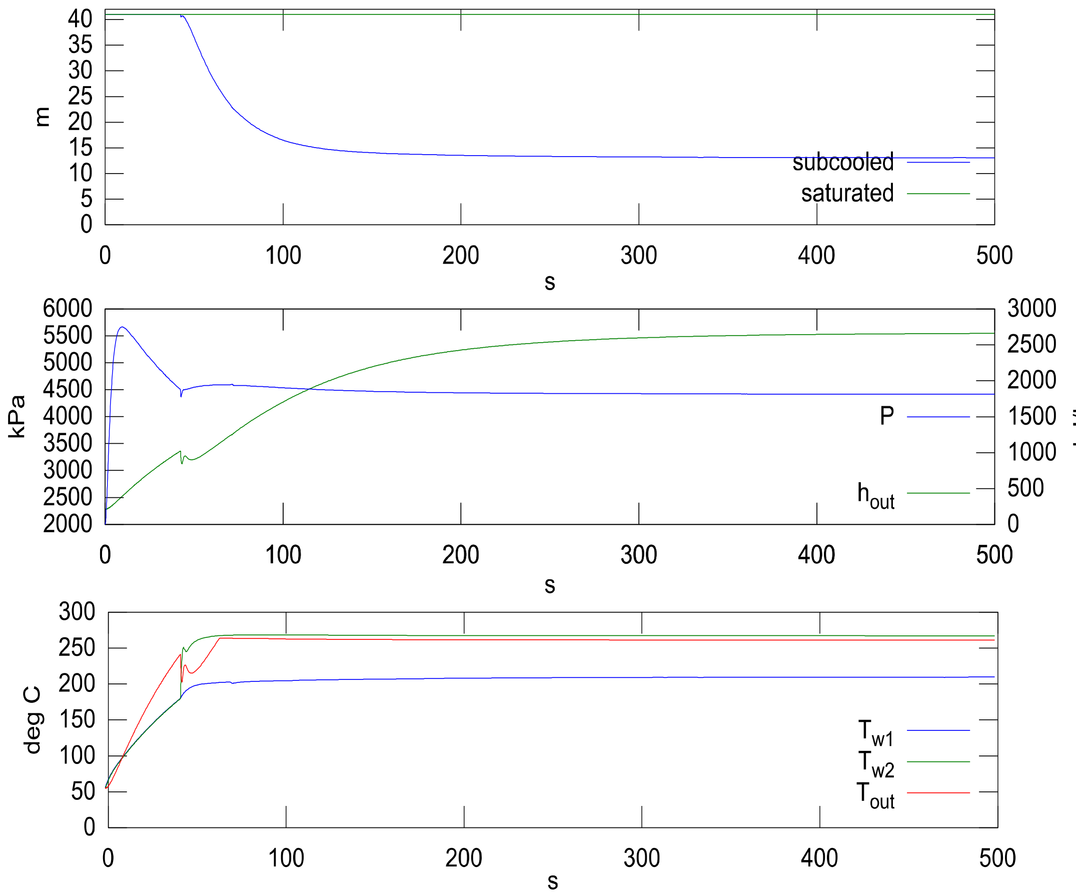

Fig.5. Dynamic simulation of the steam cavity receiver middle section when subject to a step change in heat flux. Top: Length of sub-cooled and saturated regions, Middle: Average tube pressure and outlet enthalpy. Bottom: Tube wall temperature for sub-cooled and saturated regions and fluid outlet temperature.

The third and final figure shows the outlet temperature for the section and the wall temperature for the receiver tube. When the receiver is sub-cooled, the tube wall temperature is linked the sub-cooled liquid. Once the model transitions to a two region model, the average temperature of the tube containing both the sub-cooled and saturated liquid is different, in accordance with the fluid gaining temperature as it travels through the receiver. The outlet temperature, calculated as a function of the outlet enthalpy and tube pressure is also depicted, showing a sharp increase at the beginning and settling into a constant outlet temperature, replicating the effect observed in the experimental run. The estimated transition point between sub-cooled liquid and saturated liquid in steady state is also in accordance with stead state experimental data.

These results are still subject to parameter calibration. The Solar Thermal Group's efforts in characterising the steam cavity receiver coupled to the 500 m^2 dish have been useful to gain insight into the behaviour of the boiling process. More work needs to be done to address issues such as heat transfer calculations, pressure drop estimations, outlet mass flow calculation and others.

3.5 Mass flow control

The main variable available to control the performance of the mono-tube steam cavity receiver is the feed-water mass-flow at every time instant. Variables such as ambient temperature, direct normal irradiance and wind speed are considered disturbances and may only be used to enhance the mass-flow control response.

The simulation presented in the previous section suggests that even though the temperature at the receiver outlet is highly nonlinear at saturation, the enthalpy of the system exhibits a more linear behaviour. If a control algorithm seeks to maximise the enthalpy change of the fluid rather than maintaining constant temperature, the dynamic model of the receiver can be used as a model based estimator of the receivers enthalpy gain. A suitable control algorithm should calculate the feedwater mass-flow required to achieve this goal in the minimum possible time.

Optimising the dynamic performance of the mono-tube steam cavity receiver with mass-flow control is part of ongoing work and exploring non-linear control algorithms for this purpose is the current focus of their work.

4 Conclusion

Ongoing work characterising the performance of the mono-tube cavity receiver used at the ANU 500 m^2 dish for direct steam generation has been presented. Experimental measurements of temperature along the tube length and ray-trace modelling are used to aid in this characterisation, and have resulted in a refinement of a dynamic simulation of the cavity receiver's performance. The refinement consists in the partition of the model into sub-models based on areas of similar geometry and relatively evenly distributed heat flux. A dynamic simulation of one of the sub-models is presented to demonstrate the current state of the ongoing dynamic simulation work.

Work continues on obtaining additional performance data from the mono-tube cavity receiver, improving the accuracy and scope of the dynamic simulations and the development of a mass-flow control algorithm.

Acknowledgements

The work described in the paper was supported by funding from the Australian Solar Institute.

References

[1] K. Lovegrove, G. Burgess, and J. Pye. A new 500 m2 paraboloidal dish solar concentrator. *Solar Energy*, 85(4):620 – 626, 2011. SolarPACES 2009.

[2] J. Zapata, K. Lovegrove, and J. Pye. Steam receiver models for solar dish concentrators: Two models compared. In *Proceedings of the SolarPACES Conference*, 2010.

[3] Greg Burgess, Keith Lovegrove, Scott Mackie, Jose Zapata, and John Pye. Direct steam generation using the sg4 500m2 paraboloidal dish concentrator. In *Proceedings of the SolarPACES Conference*, 2011.

[4] J.M. Jensen and H. Tummescheit. Moving boundary models for dynamic simulations of two-phase flows. In *Proc. of the 2nd Int. Modelica Conference*, 2002.

[5] J. Zapata, K. Lovegrove, J. Pye, and G Burgess. Direct steam generation with dish concentrators. In *Proceedings of the AUSES Conference*, 2010.

[6] Thomas Treichl. ODEPKG, a package for solving ordinary differential equations and more., June 2011. Last accessed 30-06-2011.

[7] Magnus Holmgren. Freeware IF97 properties for water and steam, July 2007. Last accessed 30-06-2011

[8] Thomas L. McKinley and Andrew G. Alleyne. An advanced nonlinear switched heat exchanger model for vapor compression cycles using the moving-boundary method. *International Journal of Refrigeration*, 31(7):1253 – 1264, 2008.